B-Side Electron Transfer Promoted by Absorbance of Multiple Photons in *Rhodobacter sphaeroides* R-26 Reaction Centers

Su Lin,* Jonathan A. Jackson, Aileen K. W. Taguchi, and Neal W. Woodbury

Department of Chemistry and Biochemistry and the Center for the Study of Early Events in Photosynthesis, Arizona State University, Tempe, Arizona, 85287-1604

Received: January 25, 1999; In Final Form: April 2, 1999

Femtosecond transient absorbance spectra of quinone-depleted *Rhodobacter sphaeroides* R-26 reaction centers in the Q_X transition region have been measured at 15 K under various excitation conditions. This study focuses on the excitation wavelength dependence and excitation intensity dependence of the formation of charge-separated states on the A- and B-side of the reaction center, judging from the bleaching of the 533 nm (B-side) and 544 nm (A-side) ground-state transitions of the reaction center bacteriopheophytins (H_A and H_B). Upon low-intensity selective excitation directly into the bacteriopheophytin Q_Y transitions (near 760 nm), bleaching of both ground-state bacteriopheophytin Q_X transitions (533 and 544 nm) appeared immediately, showing that initially either the A- or B-side bacteriopheophytin could be excited. However, both excited states ultimately resulted in $P^+H_A^-$ formation under these conditions. Low-intensity excitation at any of the various wavelengths (595, 750, 760, and 880 nm) showed no difference in the kinetics of the A-side charge separation forming $P^+H_A^-$ and no substantial formation of the B-side charge-separated state, $P^+H_B^-$. In contrast, high-intensity 595 nm excitation resulted in substantial long-lived bleaching of the B-side bacteriopheophytin ground-state transition at 533 nm. This 533 nm bleaching was formed with essentially the same time constant as the bleaching at 544 nm due to A-side charge separation. Both bleaching bands persisted at the longest times measured (hundreds of picoseconds) in quinone-removed reaction centers. The long-lived bleaching at 533 nm using high-intensity excitation most likely represents the formation of $P^+H_B^-$ with a relative yield (percent of total charge separate state) of nearly 40%. One possible mechanism for B-side electron transfer is that two-photon excitation of the reaction center resulting in the state $P^*B_B^*$ makes $P^+B_B^-$ thermodynamically accessible.

Introduction

One of the most interesting aspects of the function of bacterial photosynthetic reaction centers is that only one of the two possible photosynthetic electron-transfer pathways is substantially utilized under normal conditions. The three-dimensional structure of this reaction center reveals a 2-fold symmetric configuration of the protein and cofactors forming two possible electron-transfer pathways.[1−4] However, charge transfer is found almost exclusively along only one of the possible pathways, denoted A (the inactive side is referred to as the B-side) (for review, see refs 5−8).

Excitation of the primary electron donor, P, in the reaction center results in electron transfer through a series of cofactors, resulting in a metastable charge-separated state that spans the membrane. The cofactors involved as electron acceptors in the electron-transfer chain in *Rhodobacter sphaeroides* reaction centers include a monomer bacteriochlorophyll, B_A, a bacteriopheophytin, H_A, and two ubiquiones, Q_A and Q_B. The first metastable charge-separated intermediate in this series of reactions is $P^+H_A^-$, which is formed with a time constant of about 3 ps at room temperature and 1.3 ps at low temperature. No detectable H_B^- has been observed spectroscopically so far from wild-type reaction centers, except through secondary photochemistry. Photopumping methods [9−11] have shown that H_B^- can be formed with a small but significant yield when both electron acceptors on the A-side, H_A and Q_A, are reduced.

The precise origins of the asymmetric electron transfer in the reaction centers are still unclear. One factor that is thought to control the directionality is the relative free energies of the charge-separated states $P^+B_A^-$ and $P^+B_B^-$. The state $P^+B_B^-$ is thought to be higher than P* in energy, while $P^+B_A^-$ is thought to be roughly isoenergetic or slightly lower than P*.[8,12−21] The cofactors on the two sides are identical in *Rhodobacter sphaeroides*. Thus, the major energetic differences must arise from the different protein environments afforded by the homologous but distantly related core subunits of the reaction center, L and M.

A double mutant of *Rb. capsulatus*, G(M201)D/L(M212)H, has shown up to 15% charge separation on the B-side.[8] One of these two mutations, L(M212)H, converts H_A to a bacteriochlorophyll, thus removing the 544 nm absorbance band and making absorbance changes in the 533 nm bacteriopheophytin transition easier to observe. The second mutation, G(M201)D, presumably increases the relative free energy of $P^+B_A^-$ in this mutant, resulting in a 5-fold decrease in the A-side electron-transfer rate. Only about 3% of H_B^- was formed in the single L(M212)H mutant, which only had the H_A replacement but no alteration in the $P^+B_A^-$ relative free energy. This study suggested the importance of the relative free energy balance between the $P^+B_A^-$ and $P^+B_B^-$ states in governing the branching ratio of A- versus B-side electron transfer.

* To whom correspondence should be addressed. E-mail: SLIN@ASU.EDU. Phone: 602-965-0675. Fax: 602-965-2747.

10.1021/jp990303j CCC: $18.00
Published on Web 05/07/1999

Other mutants have been created that give qualitatively consistent results. A series of large-scale mutants have been constructed to increase the symmetry of protein environment around the cofactors on the A- and B-side by exchanging large fragments of the C/D, D, and E helicies between the M and L subunits.[22,23] As much as 10−20% B-side electron transfer was estimated from the transient spectral changes in the Q_X transition region in selected symmetry mutants. Again, the sites of these mutations were consistent with a variation of the relative levels of $P^+B_A^-$ and $P^+B_B^-$.

A more general understanding of how the protein environment contributes to the electrostatic potentials that control reaction directionality in the reaction center has come from both theoretical and experimental avenues. Electrostatic calculations of charge-separated-state free energies in the protein suggest that the protein sets up a strong static field resulting from charged and polar groups that favor A-side electron transfer.[21] The effective dielectric constant of the protein complex around two branches was determined from Stark effect spectral measurements.[24] The results reveal a significant asymmetry in the effective dielectric strength of the protein matrix along the two potential electron-transfer pathways, which favors the A-side. These findings are consistent with the concept that the directionality of electron transfer is governed at least in part by the effect of the protein on the relative free energies of the A- and B-side charge-separated states.

If it is largely the high free energy of $P^+B_B^-$ relative to P* that controls the rate of B-side electron transfer in the reaction center, it might be possible to overcome this barrier by initiating electron transfer from excited states with higher energy than the lowest excited singlet state of P, possibly by excitation of the reaction center with multiple photons. In this study, the effects of multiphoton excitation on electron-transfer asymmetry are investigated using high-intensity pump pulses and monitoring low-temperature absorbance changes in the Q_X transition region near 540 nm where the spectral changes are primarily contributed by H_A (544 nm) and H_B (533 nm) in the carotenoidless R-26 reaction centers.[8,23,25]

Materials and Methods

Rhodobacter sphaeroides. R-26 reaction centers were prepared following the procedure of Feher and Okamura.[26] Q_A and Q_B were then removed by treatment with 4% *N*,*N*-dimethyldodecylamine-*N*-oxide (LDAO) and *o*-phenanthroline.[27,28] Samples were suspended in a solution containing (TLE, 0.025%) 10 mM Tris-HCl (pH 8.0), 1 mM EDTA (pH 8.0), and 0.025% LDAO mixed with glycerol (1/2 v/v). The sample was placed between two glass plates with a rubber spacer of 1.2 mm, then attached to the coldfinger of a closed circulated helium displex (APD) and cooled to 15 K. Typical optical density of the sample was 2 in the sample holder at 800 nm and 15 K.

The femtosecond transient absorption spectrometer has been described previously.[29,30] Laser pulses were provided by an amplified Nd:YAG pumped rhodamine 590 dye laser. The pulse duration was 150−200 fs, and the spectral width was 5−8 nm at a repetition rate of 540 Hz. The polarization of the probe beam spectral continuum was set at the magic angle with respect to that of the excitation beam.

Spectral dispersion correction and global kinetic analysis were carried out as described previously.[29,30]

Results

Transient absorption change spectra were recorded in the bacteriopheophytin Q_X transition region from 480 to 580 nm.

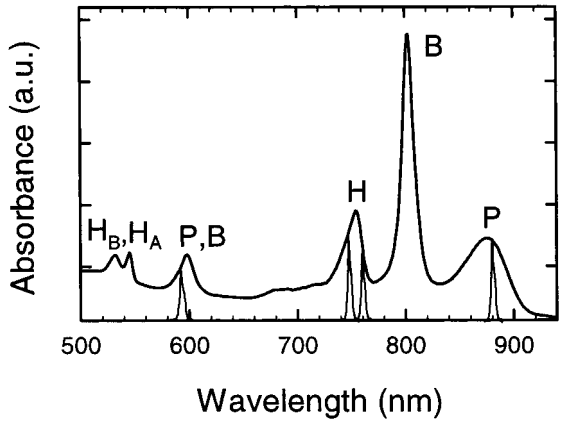

Figure 1. Ground-state absorption spectrum of *Rb. sphaeroides* R-26 at 20 K with 1 nm spectral resolution. The narrow bands are the spectra of the excitation pulses used at 595, 750, 760, and 880 nm.

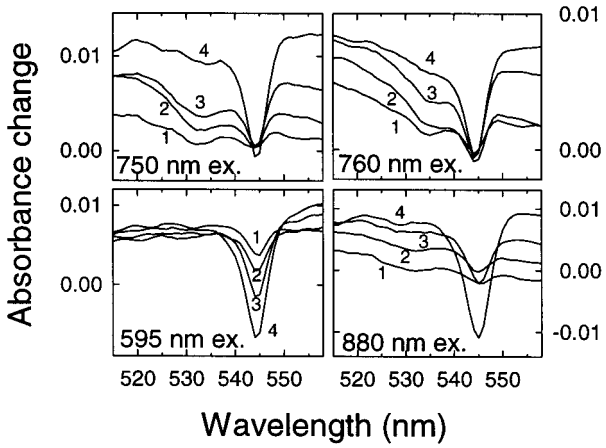

Figure 2. Early time absorbance change spectra of R-26 at 15 K in the bacteriopheophytin Q_X transition region with excitation at 750, 760, 595, and 880 nm. Spectra were recorded over a 9.5 ps time scale with a 95 fs interval between each time point and a spectral resolution of 1 nm. The spectra marked 1 were recorded at the earliest time when a significant signal was present (part way through the excitation pulse). The spectra labeled 2, 3, and 4 in each panel were recorded about 200 fs, 600 fs, and 1.4 ps after the first spectrum.

Figure 1 shows the low-temperature ground-state absorption spectrum of R-26 reaction centers and the spectral profiles of the pump pulses at the various excitation wavelengths used. The 880 nm pump pulses excite the Q_Y transition of P. Excitation at 750 and 760 nm preferentially excite the Q_Y transitions of H_B and H_A, respectively. Excitation pulses at 595 nm are predominantly absorbed by the higher energy side of the Q_X transition band of all four bacteriochlorophyll *a* molecules (the dimer P, B_A, and B_B). The 595 nm excitation pulses are directly from the amplified dye laser output, and their intensity can be varied over more than 2 orders of magnitude while still giving rise to measurable absorbance changes.

Early Time Spectral Evolution Showing Rapid Excitation Energy Redistribution. Absorbance changes in the Q_X transition region of H bands were recorded over a 9.5 ps time scale with a time resolution of 95 fs per step using excitation at 595, 750, 760, and 880 nm. Excitation intensities at the various wavelengths were adjusted in such a way that the absorbance decrease at 544 nm after 9.5 ps was roughly the same in each sample. Absorbance change spectra at early times are plotted in Figure 2. Perhaps the most systematic way of defining time zero in time courses taken using different excitation wavelengths is to monitor the absorbance change directly at the excitation wavelength. Since the excitation wavelengths used in the

measurements were not included in the probe wavelength region, the relative position of time zero using different excitation wavelengths could not be determined as precisely as desired. Thus, the times given in different panels of Figure 2 may not correspond exactly to one another. Spectra 1−4 shown in Figure 2 represent the absorbance changes within the first 1.5 ps upon laser excitation.

By use of excitation at 595 and 880 nm, an absorbance increase over a broad wavelength region was observed at very early times. This absorbance increase presumably originates from the excited-state absorption of B and/or P. A narrow bleaching at 544 nm then grows in with a time constant of about 1.5 ps. The spectral profile of the 544 nm bleaching is asymmetric because of a shoulder on the shorter-wavelength side.

When either the A- or B-side bacteriopheophytin is excited preferentially (using 760 or 750 nm pulses, respectively), the initial absorbance change exhibits ground-state bleaching of the 533 and 544 nm transitions superimposed on the broad absorption increase spectra. The 533 nm bleaching largely diminishes within 1.5 ps, while the 544 nm bleaching increases further at later delay times. Though one cannot exclusively excite just the A- or B-side bacteriopheophytin, excitation at 750 nm induces more initial bleaching at 533 nm than does 760 nm excitation (Figure 2). The rapid recovery of the 533 nm bleaching using either 750 or 760 nm excitation reflects fast energy transfer from the B-side bacteriopheophytin to the neighboring bacteriochlorophyll monomer and then to P, as has been observed previously in the Q_Y transition region at 12 K.[31]

Excitation Wavelength Dependence of $P^+H_A^-$ Spectra in the Q_X Region at Low Excitation Intensity. Spectra taken at 8 ps using the four different excitation wavelengths are compared in Figure 3a. The spectra obtained using the different excitation wavelengths have been normalized such that the differences between the minimum and maximum absorbance changes in each spectrum are the same. In general, there is very little excitation wavelength dependence of the spectral characteristics of the charge-separated state formed after 8 ps in the 520−560 nm region. All spectra exhibit similar features, showing a narrow bleaching at 544 nm superimposed on top of a broad absorption increase. The 8 ps spectrum using 880 nm excitation is slightly different from the others. The major bleaching is about 1 nm broader on the longer-wavelength side and shows less shoulder on the shorter-wavelength side, compared to 595, 750, and 760 nm excitation.

According to previous measurements of energy and electron transfer at low temperature in the Q_Y transition region, the excitation energy transfer from H to B to P occurs within a few hundred femtoseconds and the formation of $P^+H_A^-$ takes about 1.2 ps.[31,33−37] Thus, the spectrum recorded at 8 ps should represent the P^+H^- state. The comparison between spectra using different excitation wavelengths in Figure 3 also shows that there is no additional B-side electron transfer when exciting H_B selectively. Figure 3b plots typical kinetic traces at selected wavelengths near the H_A ground-state Q_X absorbance band using 880 nm excitation. The smooth lines are the fitting curves with two exponential decays of 1.2 ps and a nondecaying component. Similar kinetic decays were found using all of the excitation wavelengths at low temperature.

Excitation Wavelength Dependence of the Q_X Absorbance Changing as a Function of Excitation Intensity. The excitation intensity dependence of the spectral changes in the Q_X region was carried out using pulse energies of 2 μJ (low intensity), 8 μJ (medium intensity), and 48 μJ (high intensity) at 595 nm.

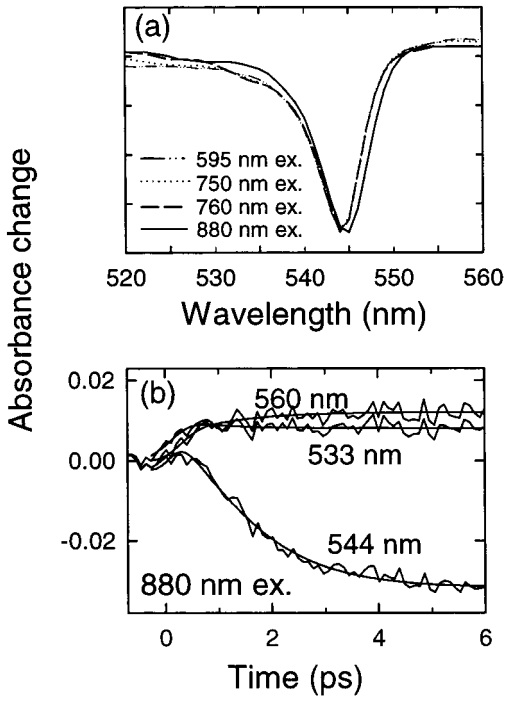

Figure 3. (a) Comparison of the 15 K time-resolved spectra of R-26 reaction centers recorded at 7.5 ± 0.5 ps after laser excitation using 595 nm (dot−dot−dashed line), 750 nm (dotted line), 760 nm (dashed line), and 880 nm (solid line) pump pulses. Spectra are scaled and offset such that both the absorbance increase around 550 nm and the bleaching around 544 nm have the same values. (b) Kinetic traces of absorbance change signals from reaction centers at 533, 544, and 560 nm using excitation at 880 nm. Data were recorded over a 9.5 ps time scale with 95 fs intervals between time points. The smooth lines are the fits obtained from a two-exponential global analysis in the wavelength region from 510 to 560 nm. The fits return a 1.2 ± 0.2 ps lifetime and a nondecaying component in each case.

The lowest excitation intensity corresponds to a photon flux of 7×10^{14} photon/cm^2, or roughly one photon was absorbed for every five reaction centers, assuming a cross section at 595 nm of 2.5×10^{-16} cm^2. Figure 4a compares the profiles of the bacteriopheophytin Q_X bands recorded at 17 ps using various excitation intensities. In addition to the 544 nm bleaching, a new bleaching near 533 nm appears using medium and high excitation intensities. Figure 4b compares the time-resolved spectra at 17 ps using the highest and lowest intensity excitation. The two spectra are normalized as described previously for Figure 3. The difference spectrum shown in the inset was calculated by subtracting the lowest intensity absorbance change spectrum from the highest intensity one. The difference spectrum is plotted with the same wavelength axis as the two 17 ps spectra but is displaced on the vertical axis for clarity. The spectral difference between high and low excitation intensity spectra is dominated by a single bleaching band at 533 nm. The kinetics with which the 533 and 544 nm bleachings appear using high-intensity excitation is the same within experimental error. Both bleachings remain for at least several hundred picoseconds.

The absorbance changes in the Q_Y bacteriopheophytin bands were also measured using the same excitation regimes that were used for the Q_X measurements (data not shown). These measurements were difficult because of the high optical density of the sample in this region and the fact that the two Q_Y bacteriopheophytin bands are so poorly resolved. Also, the absorbance changes near the 800 nm bacteriochlorophyll band are quite intensity-dependent when 595 nm excitation is used (unpublished observations), and this also complicates the

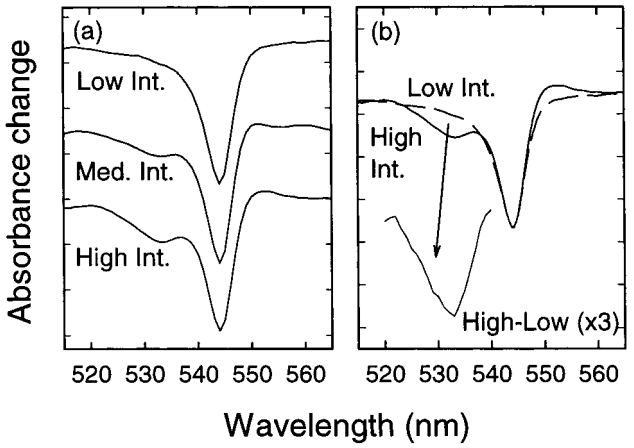

Figure 4. (a) Comparison of the time-resolved spectra 17 ps after excitation with low-intensity (upper curve), medium-intensity (4-fold stronger, middle curve), and high-intensity (24-fold stronger, lower curve) pump pulses at 595 nm. The vertical axis is plotted using arbitrary units, and the curves are offset for ease of comparison. The lowest excitation intensity corresponds to 7×10^{14} photon/cm^2 per pulse. (b) Comparison of time-resolved spectra taken at 17 ps using the lowest and the highest excitation intensities. The two spectra were aligned at 510 nm by introducing an offset and then normalized at the bleaching maximum (544 nm). The inset shows the spectral difference induced by high excitation intensity, calculated by subtracting the low-intensity spectrum from the high-intensity one. The double difference spectrum is displayed on the same wavelength axis as the main figure.

TABLE 1: Fitting Parameters Used in Figure 5

$$F(\lambda) = a_0 + a_1\, e^{-2.77[(\lambda-533)/b_1]^2} + a_2\, e^{-2.77[(\lambda-538)/b_2]^2} + a_3\, e^{-2.77[(\lambda-544)/b_3]^2}$$

excitation intensity	a_0 (AU)	a_1 (AU)	b_1 (nm)	a_2 (AU)	b_2 (nm)	a_3 (AU)	b_3 (nm)
ground state	−0.001	0.033	12.9	0.004	7.8	0.04	7.9
L intens	0.003	−0.003	13.0	−0.005	4.9	−0.03	6.0
M intens	0.031	−0.013	15.7	−0.007	8.0	−0.072	5.0
H intens	0.023	−0.023	13.4	−0.006.	7.2	−0.075	5.2

interpretation of the rather small amplitude spectral changes observed near 760 nm upon $P^+H_A^-$ formation. However, the changes observed in this spectral region are consistent with those shown for the Q_X region, showing a broader bleaching spectrum after 17 ps than is observed using low-intensity excitation, particularly on the short-wavelength side, as one would expect if both bacteriopheophytins were reduced at this time.

The ground-state absorbance spectra in the Q_X spectral region and the absorption difference spectra at 17 ps from Figure 4 were fit with Gaussian spectral profiles in order to quantitate the relative amount of bleaching at 544 and 533 nm as a function of excitation intensity. The ground-state and absorbance change spectra using all excitation intensities can be fit well with three Gaussian bands centered at 533, 538, and 544 nm. The fitting parameters are listed in Table 1. Figure 5 shows the ground-state absorption spectrum and absorbance change spectra using various 595 nm excitation intensities as well as the results of the spectral deconvolutions. The dashed lines in each panel of Figure 5 peaking at 544 nm are the sum of both the 538 and 544 nm Gaussian bands resulting from the fit. As can be seen from Table 1, the amplitude of the 538 nm Gaussian remains about one-tenth that of the 544 nm Gaussian in both the ground-state spectrum and the bleaching spectra at each excitation intensity. Thus, the 544 and 538 nm Gaussians were considered to both be components of the ground-state band of H_A. A constant was also added in the spectral fitting to compensate the broad absorption increase in this spectral region. The results of the Gaussian fits in Figure 5 show that the amplitude of the

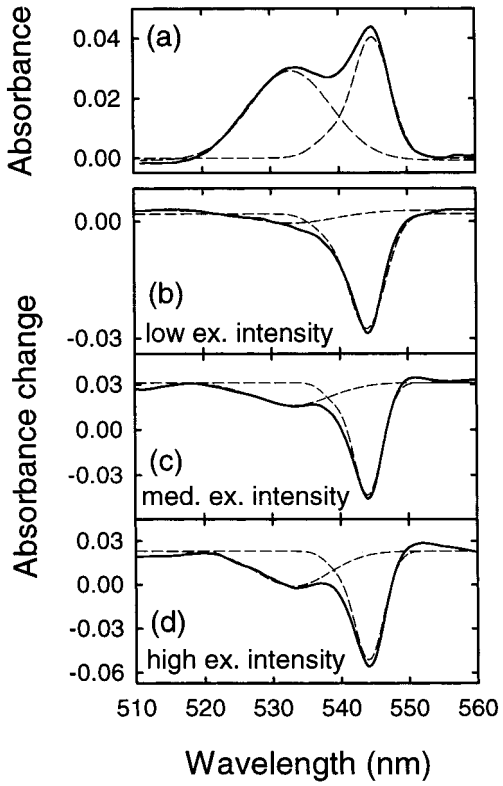

Figure 5. Deconvolution of spectra into Gaussian components obtained by fitting (a) the ground-state and time-resolved absorption spectra using (b) low, (c) medium, and (d) high intensities of 595 nm excitation. Fitting parameters are listed in Table 1, and excitation intensities are those given in Figure 4.

533 nm bleaching increases dramatically relative to that of the 544 nm bleaching as the excitation intensity increased.

The total areas of the 533 and 544 nm Gaussian fitting components are plotted as a function of excitation intensity in Figure 6. The bleaching areas are calculated directly from the fitting parameters listed in Table 1 and are normalized to the areas of the corresponding Gaussian fitting components for the ground-state band. This gives a quantitative comparison of the fraction of the 533 and 544 nm bands bleached at each excitation intensity. The 544 nm band shows almost the same amount of bleaching at the two higher excitation intensities, while the 533 nm band increases by more than 50% between the medium and high excitation intensities.

Discussion

Fast Energy and Electron Transfer as a Function of Low-Intensity Excitation at a Variety of Wavelengths. There have been a number of femtosecond time-resolved spectroscopic studies of energy transfer in reaction centers using selective excitation of the bacteriopheophytin and monomer bacteriochlorophyll cofactors in the Q_Y transition region both at room temperature[30,32,38−42] and at low temperatures.[31,33,36,37,43] The results consistently show rapid excitation energy transfer from H to B to P on the time scale of hundreds of femtoseconds. Energy transfer is essentially complete within 500 fs of the excitation, though spectral differences persist on a much longer time scale, which could be indicative of either excitation wavelength-dependent photochemistry or of spectral heterogeneity in the reaction center population.[31,36,37] Energy transfer along the two branches of cofactors in the reaction center has previously been compared using a mutant L(M214)H (the β-mutant) in which the bacteriopheophytin on the A-side was

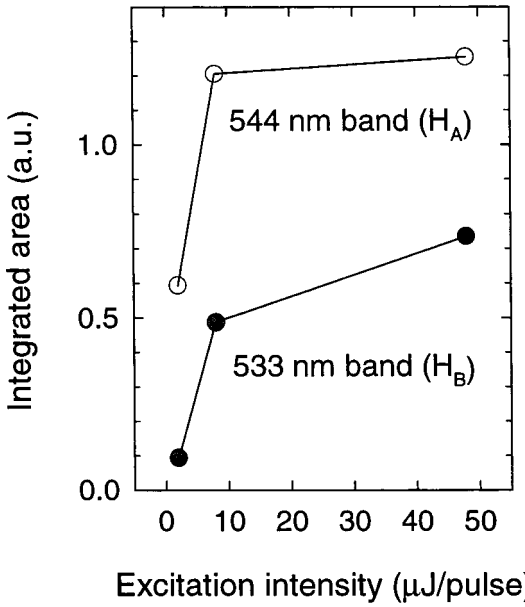

Figure 6. Area of 533 and 544 nm absorbance decrease bands from the transient spectra of Figure 5 plotted as a function of excitation intensity. The total area of each spectral component is calculated from the Gaussian fits of Table 1. The analytical expression for the area of a Gaussian is $\int a\ e^{-(x/c)^2}\ dx = (\sqrt{\pi}/2)ac$, where $c = b/[2(\ln 2)^{1/2}]$ and b is the half-width of the Gaussian curve. Thus, the area is simply proportional to ab, and this product was used to calculate the relative areas and each of the Gaussian components of the bleaching spectra. These areas were normalized to the area of the corresponding Gaussian component of the ground-state spectrum.

replaced by a bateriochlorophyll in order to better resolve the optical transitions associated with cofactors on the two branches.[43] It was concluded from this that there is little difference in the rate of energy transfer along the two sides.

In the present study, the fate of excitations in the Q_X region at 595 nm has been investigated and compared to excitation in the Q_Y region. Figure 2 shows that a recovery of the ground-state bleaching at 533 nm takes place in hundreds of femtoseconds when H_B is preferentially excited with low-intensity pulses at 750 nm, presumably because of fast energy transfer to other cofactors. When reaction centers are excited preferentially in the H_A transition at 760 nm, the bleaching at 544 nm remained for nanoseconds, presumably because of the fact that the decay of H_A* and the appearance of H_A^- occur on a similar time scale at low temperatures, and thus, the ground-state band of H_A remains bleached. These results are consistent both with the accepted notions of rapid energy transfer away from the bacteriopheophytins and with unidirectional charge separation along the A-branch. There is no evidence in the Q_X region of the spectrum for formation of charge-separated states other than $P^+H_A^-$ using low excitation intensity. In fact, all excitation wavelengths result in very similar spectral changes after 5 ps (Figure 3). There are some variations in the 544 nm spectral bandwidth, probably due to conformational heterogeneity of the reaction center on this time scale.[29,31]

533 nm Bleaching at High Excitation Intensity Likely Reflects H_B^- Formation. When reaction centers were excited with higher laser intensities at 595 nm (each RC absorbs 0.8 photons on average at medium intensity or nearly 5 photons on average at high intensity), a pronounced bleaching of the ground-state absorbance near 533 nm is observed (Figure 4). The amplitude of the 533 nm bleaching increases with increasing excitation intensity and shows a different dependence on excitation intensity than does the extent of the 544 nm bleaching (Figure 6). Because the magnitude of the bleaching at 533 nm is small and is superimposed on top of a broad absorption increase, an accurate determination of the formation and decay kinetics of this feature is difficult. However, from a comparison of the size of the bleaching at 533 and 544 nm, it appears that the two signals have comparable formation time constants and both have decay constants longer than the longest time scale measured. As shown above, the excited state of H_B lives less than 1 ps. Therefore, the long-lived bleaching (longer than 100 ps) formed under high excitation intensities is unlikely to be due to an excited state of H_B. A much more likely possibility is that this spectral feature is due to the formation of H_B^-.

If this new state formed at high-intensity involves H_B^-, then what is the donor? The most likely candidates are either P or B_B. One would expect to distinguish between the two possible states from absorbance changes in the Q_Y region. However, this is complicated by the fact that the absorbance changes near 800 nm are very sensitive to the excitation wavelength, excitation intensity, and details of the sample preparation.[31,37] In addition, since this state is not kinetically resolved from $P^+H_A^-$, the absorbance changes associated with $P^+H_A^-$ underlie the absorbance changes for the state involving H_B. The electrochromic shift of the B-band near 800 nm is also apparently much smaller owing to the formation of the $P^+H_B^-$ state than to $P^+H_A^-$,[45] making it difficult to detect. For these reasons, it has not been possible to unambiguously determine the Q_Y spectral characteristics of the new high-intensity state. However, it seems very likely that at least on long time scales (hundreds of picoseconds) the cation resides on P simply because P^+ is clearly the most stable cation state for A-side electron transfer and there is no reason to believe that the energies of neighboring cofactors are so radically altered upon B-side electron transfer that the identity of the most thermodynamically stable cation formed would be different.

Possible Mechanisms for B-Side Electron Transfer at High Excitation Intensity. The excitation intensity dependence of formation of H_B^- suggests that it is generated through a two-photon process. Two-photon absorption can occur as a two-step process with one photon being absorbed in each step or as a true two-photon transition. Three possible models for B-side electron transfer from two-photon excited states are considered below.

One possibility is that $P^+H_B^-$ is generated by sequential absorption of one photon by P, which results in normal $P^+H_A^-$ formation, and then one by B_B, resulting in $B_B^+H_B^-$ formation. However, this model suffers from the fact that it requires the stable formation of $B_B^+H_B^-$ in the same reaction center as $P^+H_A^-$. It also requires that charge separation compete with annihilation if P and B_B are simultaneously in the excited state (which is likely, given the short pulse) or that charge separation from B_B* compete with energy transfer to P^+ if $P^+H_A^-$ has already been formed when B_B is excited. Previous measurements that have attempted to measure $B^+H_B^-$ formation from B* (on either the A- or B-side) have indicated that the lifetime of any B^+H^- state formed is much shorter than that of the $P^+H_A^-$ state, on the order of picoseconds or less.[30,31,36] It is also not clear that the charge-separated state $B_B^+H_B^-$ is energetically more stable than B_B*. A study of a mutant with the P-band completely depleted, VR(L157), does not appear to form any $B_B^+H_B^-$ (or $B_A^+H_A^-$ for that matter) when B is excited directly at 800 nm even though B* lives for many hundreds of picoseconds.[46]

Another possible mechanism is that H_B^- is formed from a doubly excited state of P, P**, generating $P^+H_B^-$. In this model, the branching ratio between A- versus B-side electron transfer

depends on whether P is excited by one photon or two. Previous studies have suggested that $P^+B_A^-$ is considerable lower in energy than that of $P^+B_B^-$, resulting in branching ratio estimates for one-photon absorption by P of more than 200:1,[11] 25:1,[47] and 30:1.[8] The large branching ratio favoring A-side electron transfer is thought to be largely due to $P^+B_B^-$ being well above P* in energy. However, if P is doubly excited forming a P** state, the branching ratio could be significantly altered compared to P* because of the higher energy available from the doubly excited state. If P** is well above both $P^+B_A^-$ and $P^+B_B^-$, then the distinction between A-side and B-side electron transfer should decrease.

This model is consistent both with the excitation intensity dependence and with the similarity in the apparent formation kinetics of $P^+H_A^-$ and the new state involving H_B (presumably $P^+H_B^-$). The formation kinetics of $P^+H_B^-$ at high excitation intensity is expected to be the same as the kinetics of $P^+H_A^-$ formation if the two pathways are competing. However, on the basis of this mechanism, one might expect to see a faster electron transfer from the P** state than from the P* state simply because it has two possible decay pathways. The global fitting analysis in the Q_X transition region returned a single formation time of 1.2 ± 0.2 ps, which is similar to the time constant of charge separation from P* forming $P^+H_A^-$ at 15 K. One also might be concerned that the lifetime of the doubly excited state would simply not be long enough to result in electron transfer before relaxing to the lowest excited singlet state of P. Our data showed a branching ratio as high as 1:1.7 for B-side vs A-side electron transfer at the highest excitation intensities, which would suggest that if this model is correct, the P** state must live long enough so that most (at least 60%) of the electron transfer could occur from it on the picosecond time scale, even assuming that both $P^+H_A^-$ and $P^+H_B^-$ can be formed from P** equally.

Alternatively, and probably more likely, the 595 nm excitation could generate B_B* and P* simultaneously, and electron transfer could occur between these two excited molecules forming $P^+B_B^-$. (Of course, a similar doubly excited state on the A-side could result in $P^+B_A^-$, but this would be indistinguishable from normal A-side photochemistry.) B*P* could undergo electron transfer from the LUMO of P^* to the now unfilled HOMO of B^* and be much more thermodynamically favored than electron transfer from the LUMO of P^* to the LUMO of B as necessarily must happen from the singly excited P^* state. To explain the 1:1.7 B- vs A-side transfer branching ratio, a minimum of $^3/_4$ of the reaction centers must have been doubly excited in P and one of the monomer bacteriochlorophylls simultaneously at high intensity, and half of these would have had to go on to form $P^+B_B^-$. This seems feasible, given that at the highest intensity, the average reaction center would have had five photons pass within its cross section and there are three different bacteriochlorophyll components to do the absorbing (B_A, B_B, and P). Also, the absorption cross section for formation of $B_A^* + B_B^*$ should be considerably higher than that for formation of P** at 595 nm, favoring the idea that the B-side electron transfer arises from P*B* rather than from P**. (This can be seen from the fact that the absorbance changes in the 590 nm region in the P^* state are small and broad, making absorption of a second photon by P^* less likely than absorption by one of the monomer bacteriochlorophylls.) Of course, this model, like the first one discussed above, does require that annihilation between P* and B* be significantly slower than electron transfer between these excited states. To further distinguish between these possibilities, two photon/two color excitation based experiments are being performed.

In summary, it appears to be possible to induce nearly 40% of electron transfer (measured as a fraction of total charge-separated state formed) along the B-branch of the bacterial reaction center using high-intensity excitation in the 595 nm region. The mechanism of this process is not yet clear but likely involves a doubly excited state of P or, more likely, of P and B that can give rise to charge separation in either direction. This is consistent with the notion that the $P^+B_B^-$ state is above both P* and $P^+B_A^-$ in energy, resulting in little B-side electron transfer from the P* state. According to this model, both of the P^+B^- states are lower than the excited state formed by two photons. The $P^+H_B^-$ state is long-lived when the reaction center quinone is removed and in that respect appears to resemble the $P^+H_A^-$ state. Additional studies of high-intensity excitation at other wavelengths or using multiple pulses should help to distinquish between possible mechanisms of B-side charge separation at high excitation intensity.

Acknowledgment. The authors thank Professor M. Gunner for helpful discussions concerning the possible mechanisms of electron transfer from doubly excited states, which substantially influenced the conclusions of this paper. This work was supported by a grant (MCB-9513457-004) from the National Science Foundation. Instrumentation was purchased with funds from NSF Grant DIR-8804992 and Department of Energy Grants DE-FG-05-88-ER75443 and DE-FG-05-87-ER75361. This is publication no. 406 from the Arizona State University Center for the Study of Early Events in Photosynthesis.

References and Notes

(1) Deisenhofer, J.; Epp, O.; Miki, K.; Huber, R.; Michel, H. *J. Mol. Biol.* **1984**, *180*, 385.
(2) Allen, J. P.; Feher, G.; Yeates, T. O.; Komiya, H.; Rees, D. C. *Proc. Natl. Acad. Sci. U.S.A.* **1987**, *84*, 5730.
(3) Chang, C.-H.; El-Kabbani, O.; Tiede, D.; Norris, J.; Schiffer, M. *Biochemistry* **1991**, *30*, 5352.
(4) Chirino, A. J.; Lous, E. J.; Huber, M.; Allen, J. P.; Schenck, C. C.; Paddock, M. L.; Feher, G.; Rees, D. C. *Biochemistry* **1994**, *33*, 4584.
(5) Kirmaier, C.; Holten, D. *Photosynth. Res.* **1987**, *13*, 225.
(6) Kirmaier, C.; Holten, D. In *The Photosynthetic Reaction Center*; Deisenhofer, J., Norris, J. R., Eds.; Academic Press: San Diego, 1993; Vol. II, p 49.
(7) Woodbury, N. W.; Allen, J. P. In *Anoxygenic Photosynthetic Bacteria*; Blankenship, R. E., Madigan, M. T., Bauer, C. E., Eds.; Kluwer Academic Publishers: Dordrecht, 1995; Vol. 2, p 527.
(8) Heller, B. A.; Holten, D.; Kirmaier, C. *Science* **1995**, *269*, 940.
(9) Robert, B.; Lutz, M.; Tiede, D. M. *FEBS Lett.* **1985**, *183*, 326.
(10) Tiede, D. M.; Kellogg, E.; Breton, J. *Biochim. Biophys. Acta* **1987**, *892*, 294.
(11) Kellogg, E. C.; Kolaczkowski, S.; Wasielewski, M. R.; Tiede, D. M. *Photosynth. Res.* **1989**, *22*, 47.
(12) Parson, W. W.; Chu, Z.-T.; Warshel, A. *Biochim. Biophys. Acta* **1990**, *1017*, 251.
(13) Finkele, U.; Lauterwasser, C.; Zinth, W.; Gray, K. A.; Oesterhelt, D. *Biochemistry* **1990**, *29*, 8517.
(14) Thompson, M. A.; Zerner, M. C.; Fajer, J. *J. Phys. Chem.* **1991**, *95*, 5693.
(15) Chan, C.-K.; DiMagno, T. J.; Chen, L. X.-Q.; Norris, J. R.; Fleming, G. R. *Proc. Natl. Acad. Sci. U.S.A.* **1991**, *88*, 11202.
(16) Kirmaier, C.; Holten, D. *Biochemistry* **1991**, *30*, 609.
(17) Shkurapatov, A. Y.; Shuvalov, V. A. *FEBS Lett.* **1993**, *322*, 168.
(18) Nagarajan, V.; Parson, W. W.; Davis, D.; Schenck, C. C. *Biochemistry* **1993**, *32*, 12324.
(19) Schmidt, S.; Arlt, T.; Hamm, P.; Huber, H.; Nägele, T.; Wachtveitl, J.; Meyer, M.; Scheer, H.; Zinth, W. *Chem. Phys. Lett.* **1994**, *223*, 116.
(20) Kirmaier, C.; Laporte, L.; Schenck, C. C.; Holten, D. *J. Phys. Chem.* **1995**, *99*, 8903.
(21) Gunner, M. R.; Nicholls, A.; Honig, B. *J. Phys. Chem.* **1996**, *100*, 4277.
(22) Taguchi, A. K. W.; Eastman, J. E.; Gallo, D. M., Jr.; Sheagley, E.; Xiao, W.; Woodbury, N. W. *Biochemistry* **1996**, *35*, 3175.
(23) Lin, S.; Xiao, W.; Eastman, J. E.; Taguchi, A. K. W.; Woodbury, N. W. *Biochemistry* **1996**, *35*, 3187.
(24) Steffen, M. A.; Lao, K.; Boxer, S. G. *Science* **1994**, *264*, 810.

(25) Kirmaier, C.; Holten, D.; Parson, W. W. *Biochim. Bhiophys. Acta* **1985**, *810*, 49.
(26) Feher, G.; Okamura, M. Y. In *The Photosynthetic Bacteria*; Clayton, R. K., Sistrom, W. R., Eds.; Plenum Press: New York, 1978; p 349.
(27) Woodbury, N. W.; Lin, S.; Lin, X.; Peloquin, J. M.; Taguchi, A. K. W.; Williams, J. C.; Allen, J. P. *Chem. Phys.* **1995**, *197*, 405.
(28) Okamura, M. Y.; Isaacson, R. A.; Feher, G. *Proc. Natl. Acad. Sci. U.S.A.* **1975**, *72*, 3491.
(29) Peloquin, J. M.; Lin, S.; Taguchi, A. K. W.; Woodbury, N. W. *J. Phys. Chem.* **1995**, *99*, 1349.
(30) Lin, S.; Taguchi, A. K. W.; Woodbury, N. W. *J. Phys. Chem.* **1996**, *100*, 17067.
(31) Lin, S.; Jackson, J.; Taguchi, A. K. W.; Woodbury, N. W. *J. Phys. Chem. B* **1998**, *102*, 4016.
(32) Breton, J.; Martin, J.-L.; Migus, A.; Antonetti, A.; Orszag, A. *Proc. Natl. Acad. Sci. U.S.A.* **1986**, *83*, 5121.
(33) Breton, J.; Martin, J.-L.; Fleming, G. R.; Lambry, J.-C. *Biochemistry* **1988**, *27*, 8276.
(34) Fleming, G. R.; Martin, J. L.; Breton, J. *Nature* **1988**, *333*, 190.
(35) Stanley, R. J.; Boxer, S. G. *J. Phys. Chem.* **1995**, *99*, 859.
(36) Van Brederode, M. E.; Jones, M. R.; Van Mourik, F.; Van Stokkum, I. H. M.; Van Grondelle, R. *Biochemistry* **1997**, *36*, 6855.
(37) Vos, M. H.; Breton, J.; Martin, J.-L. *J. Phys. Chem. B* **1997**, *101*, 9820.
(38) Jia, Y.; Jonas, D. M.; Joo, T.; Nagasawa, Y.; Lang, M. J.; Fleming, G. R. *J. Phys. Chem.* **1995**, *99*, 6263.
(39) Haran, G.; Wynne, K.; Moser, C. C.; Dutton, P. L.; Hochstrasser, R. M. *J. Phys. Chem.* **1996**, *100*, 5562.
(40) Jonas, D. M.; Lang, M. J.; Nagasawa, Y.; Joo, T.; Fleming, G. R. *J. Phys. Chem.* **1996**, *100*, 12660.
(41) Wynne, K.; Haran, G.; Reid, G. D.; Moser, C. C.; Dutton, P. L.; Hochstrasser, R. M. *J. Phys. Chem.* **1996**, *100*, 5140.
(42) Breton, J.; Martin, J.-L.; Migus, A.; Antonetti, A.; Orszag, A. In *Ultrafast Phenomena V*; Fleming, G. R., Siegman, A. E., Eds.; Springer-Verlag: 1986; p 393.
(43) Stanley, R. J.; King, B.; Boxer, S. G. *J. Phys. Chem.* **1996**, *100*, 12052.
(44) Van Brederode, M. E.; Jones, M. R.; Van Grondelle, R. *Chem. Phys. Lett.* **1997**, *268*, 143.
(45) Zhou, Q.; Mattioli, T. A.; Robert, B. In *Reaction Centers of Photosynthetic Bacteria*; Michel-Beyerle, M.-E., Ed.; Springer-Verlag: New York, 1990; Vol. 6, p 11.
(46) Jackson, J. A.; Lin, S.; Taguchi, A. K. W.; Williams, J. C.; Allen, J. P.; Woodbury, N. W. *J. Phys. Chem. B* **1997**, *101*, 5747.
(47) Bixon, M.; Jortner, J.; Michel-Beyerle, M.-E. *Biochem. Biophys. Acta* **1989**, *977*, 273.